# Mechanical Characterisation of the Four Most Used Coating Materials for Optical Fibres

Yazmin Padilla Michel[1,3], Massimiliano Lucci[2], Mauro Casalboni[3],
Patrick Steglich[1,3] and Sigurd Schrader[1]
[1]*Faculty of Engineering and Natural Sciences, Technical University of Applied Sciences Wildau, Wildau, Germany*
[2]*Dept. of Physics, University of Rome "Tor Vergata", Rome, Italy*
[3]*Dept. of Industrial Engineering, University of Rome "Tor Vergata", Rome, Italy*

Keywords: Fibre Optics, Coating Materials, Young's Modulus, Nanoindentation, Attenuation.

Abstract: Optical multimode fibres have a wide variety of applications ranging from industrial to medical use. Therefore, even if they are just used as waveguides or sensors, it is important to characterise the whole fingerprint, including the optical and mechanical properties of such fibres. Since the stiffness/elasticity of a material could influence the optical output of a fibre due to micro-bendings, in this paper we report the calculated Young's Modulus of acrylate, fluorinated acrylate, polyimide and silicone, which are the four most used coating materials for such optical components. The results demonstrate that Young's Modulus does have an impact on the attenuation of propagating light along the optical fibre. However, the refractive index of the coating materials still has a significant impact on the performance of optical fibres.

## 1 INTRODUCTION

There is a large list of publications from a diverse scientific area, explaining the relation between fibre's throughput and its deformation, e.g. torsion, strain and bending (Gambling, et al. 1978; Murakami and Tsuchiya, 1978; Valiente and Vassallo. 1989; Badar, et al. 1991; Badar and Maclean, 1991; Boechat, et al. 1991; Renner, 1992; Faustini and Martini, 1997; Durana, et al. 2003; Wang, Farrell and Freir, 2005; Kovacevic and Nikezic, et al. 2006; Wang, et al. 2007; for mentioning some of them). Fibre characterisation in the literature has been performed by only considering the core and cladding of the optical fibre, while the influence of the coating (i.e. the protective third polymeric layer of optical fibres) on the light transmission in the optical fibres has been fully ignored.

With the increasing number of applications of fibre-based devices in the chemical industry, spectroscopy, and life sciences (where the NIR spectrum is of high importance); besides the constant emergence of new materials; the mechanical and optical characterisation of coating materials is of great importance and must be included into the theoretical models.

In 2002 Corning Incorporated recognised the lack of public information about their fibre coatings and released in a white paper the Young's Modulus and performance of their UV-cured dual-layer optical fibre coatings and its performance (Mitra, Kouzmina and Lopez, 2010). In Padilla Michel, et al (2012), it is proved that there is a strong dependency between coating materials and the optical output of multimode fibres (MMF) optimised for VIS-NIR spectrum. In the same proceeding it is concluded that, regardless of the bending diameter, the refractive index of the fibre coating is a determining factor for fibre throughput. Their results also show that when the coating refractive index is higher than that of the cladding, the attenuation increases considerably, while it is negligible when it is lower.

From the experiment reported in the present paper, we have obtained the Young's Modulus ($E$) of the same four coating materials tested by Padilla Michel, et al. (2012), which will be useful to understand and develop more realistic fibre optics models. Furthermore, we have proved that the $E$-value of the coatings affects the performance of the optical fibres. However, the refractive index is a dominant parameter which determines the throughput of a coated MMF.


Padilla Michel Y., Lucci M., Casalboni M., Steglich P. and Schrader S..
Mechanical Characterisation of the Four Most Used Coating Materials for Optical Fibres.
DOI: 10.5220/0005336700960102
In *Proceedings of the 3rd International Conference on Photonics, Optics and Laser Technology* (PHOTOPTICS-2015), pages 96-102
ISBN: 978-989-758-092-5

## 2 MATERIALS AND METHODS OF MEASUREMENT

For the present test, the following materials and devices were used:

- A Nanoindenter (NanoTest from Nano Materials Ltd., Wrexham, UK) shown in Figure 1.
- 5 fibre holders consisting of a 20 mm x 20 mm x 5 mm plate made of aluminium and each of them has 5 grooves engraved (see Figure 2).
- Fast curing glue (cyanoacrylate).
- 5 aluminium posts (see Figure 1, right).
- 5 fibre samples of each material listed in Table 1. The length of each fibre sample is 1 cm (total 25 fibres samples of 1 cm length).

Table 1: Fibre parameters provided by FibreTech GmbH (Berlin, Germany). The material of the fibre's core was fused silica and that of the cladding was fluorinated fused silica. The refractive indices of the preform were given by the manufacturer (Heraeus Suprasil®) at λ=600 nm.

| Coating Materials | Core ($n_1$) | Clad ($n_2$) | Coating ($n_3$) | Core/Clad/Coating outer diameters [µm] |
|---|---|---|---|---|
| Single-coated acrylate | 1.458 | 1.442 | 1.49 | 200/240/380 |
| Double-coated acrylate | 1.458 | 1.442 | 1.505 (I)<br>1.541 (II) | 200/240/375 |
| Fluorinated acrylate | 1.458 | 1.442 | 1.414 | 200/240/350 |
| Polyimide | 1.458 | 1.442 | 1.7 | 200/240/264 |
| Silicone | 1.458 | 1.442 | 1.409 | 200/240/306 |

Considering that the thickness of the studied coatings in this paper range from 12 µm to 70 µm and that the materials are elastic ($E$ in the order of MPa for polymers) compared to the cladding (71.7 GPa) the measurement of $E$ was not straightforward and several parameters had to be considered.

For the indenter, a Berkovich tip, i.e. a three-sided diamond, was used. Thermal effects were minimised using a temperature controller set at 23 °C. The Nanoindenter was mounted on an anti-vibrational table to minimize the disturbances. In Olson (2002), it is shown that the lower the $E$-values to be measured, the greater the contact depth should be. Hence for materials where $E$ is in the order of MPa, the indent should have at least 1 µm of depth to consider the measurement to be accurate. Also considering all the errors and trials reported in Olson (2002), and the dimensions of the outer diameter of our samples, we decided not to polish the coatings (i.e. the side-polishing of the fibres), to keep the coating surface as smooth and uniform as possible.

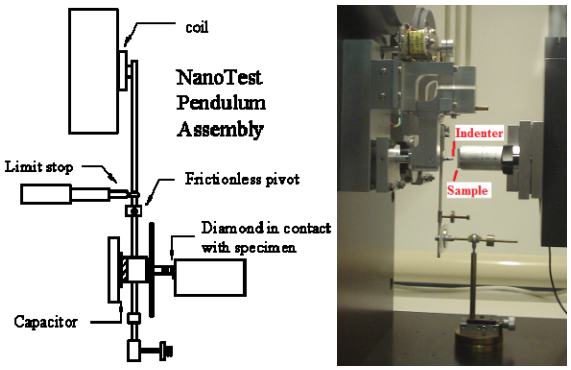


Figure 1: On the left, a schematic showing the main components of the Nanoindenter (the schematic was taken from the NanoTest specifications brochure). On the right, a picture of the machine with a mounted sample is shown.

Batches of five fibres of the same coating were glued onto an aluminium plate (see Figure 2) using a minimum amount of cyanoacrylate. Once the sample was mounted on the XYZ-stage of the nanoindenter (see Figure 1), it is important to carefully select the area to be used for indentation, which for our experiment is an array of 3x10 indents. The indents were made very close to each other (separation of 15 µm), so that, the entire array was clearly focused with the microscope. Thus, we minimise miscalculations of the maximum depth of the indents.

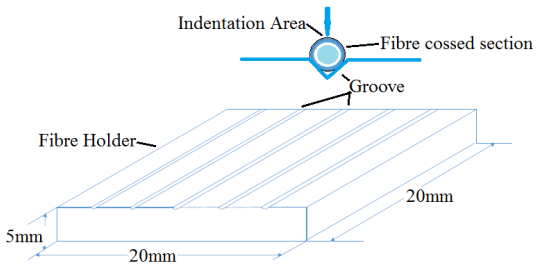


Figure 2: Schematic of the aluminium plate used for holding the fibres and a cross-section of an optical fibre mounted on a groove. The indentation area is on top of the fibre centre.

After choosing the area for indentation, the machine creates a "Contact Compliance vs Voltage" curve to show where the inflexion point occurs. This is an important parameter because it is taken as the zero-point to measure the indent depth and calculate its contact area. From the accuracy of this measurement depends the over- or underestimation of $E$. The measurements were repeated two or three times and a total of 330 indents were done on the samples mentioned in Table 1.

### 2.1 Available Public Data

As mentioned in section 1, there are few publications regarding $E$ of the fibre's coating materials. Some available public data for acrylate coatings are listed in Table 2. These data were used as reference to verify the validity of our results.

Table 2: Published $E$-values of acrylate coatings.

| Author | Young's Modulus of double and single coated acrylate [MPa] | | |
|---|---|---|---|
| | Outer Coating | Inner Coating | Single Coating |
| Mitra, et al. (2010) | 650 – 950 | 1 – 1.7 | ~ 1500 |
| Olson (2002) | 763 – 1043 | 3.29 – 5.06 | 36.8 – 60.4 |

## 3 ANALYSIS AND RESULTS

Every time a measurement is finished, the software of the Nanoindenter (NanoTest NT1) shows an indentation review with a "Load vs Depth" curve together with the calculated Reduced Modulus ($E_r$) and other parameters such as Hardness ($H$), Elastic Recovery, Contact Compliance and the respective statistical errors.

The parameters $H$ and $E_r$ are calculated from the tangents slope of the resulting unloading curve. The following equation development is taken from Olson (2002). On one hand, $H$ is defined as: $H=P/A_r$, where $P$ is the Maximum Load and $A_r$ is the Residual Indentation Area. For our measurements, $P$=5±0.2 mN was used. On the other hand, the quantity $E_r$ relates the $E$-values of the indenter and the sample as follows:

$$E_r = \frac{E_s E_i}{E_i(1-\nu_s{}^2) + E_s(1-\nu_i{}^2)} \quad (1)$$

where $\nu$ is the Poisson's Ratio, $E_s$ and $E_i$ are the $E$-values of the sample and indenter, respectively. From equation 1 we isolate $E_s$, as follows:

$$E_s = \frac{(E_s E_i)(1-\nu_s{}^2)}{E_i - E_r(1-\nu_i{}^2)} \quad (2)$$

The $\nu$-values range normally between 0 and 0.50 (for majority of materials), being 0.50 the value for perfectly elastic materials such as rubber, hence we have taken $\nu$=0.50 for silicone coating. The $\nu$-values of single coating acrylate ($\nu$=0.49) and double coating acrylate ($\nu$=0.44) are taken by averaging the values from Olson (2002). The value $\nu$=0.34 of polyimide was provided by the manufacturer DuPont™. For fluorinated acrylate the used value is $\nu$=0.37. This procedure is to extrapolate $E$ from $E_r$.

Finally, from equation 2, we obtained the final $E_s$ of each material as shown in the following subsections.

### 3.1 Double-coated Acrylate

Double coated acrylate coating is a typical UV-cured dual layer of urethane-acrylate oligomers consisting of a very elastic inner acrylate and a second outer layer of stiffer acrylate (see Table 2). Since we have not polished the coatings, only the $E_r$ of the outer coating was measured. As shown in table 1, the fibre manufacturer has provided only the specification of the outer diameter of the fibre, while there is no information about the inner coating diameter being provided. Therefore we have made the very superficial indents of approximately 1 µm of depth, assuming that the outer coating thickness is much thicker than 1 µm.

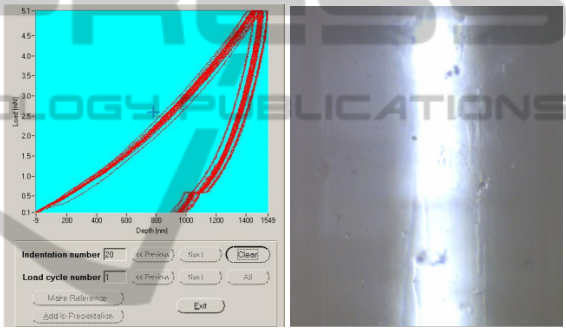


Figure 3: On the left, snapshot of the 20 best loading curves. On the right, a picture of the area selected after indentation, the material is so elastic that the indents are not visible.

Figure 3 shows the results of the best nanoindentations made on this coating. We discarded those curves affected by error, i.e. scratches or contaminants on the surface. The average of the 20 selected curves (Figure 3, left) is $E_r$=2572±57 MPa and the average Maximum Depth *(MD)* is 1507±27 nm, these values are comparable to that given in Table 2. Substituting this value into equation 2 we obtained $E_s$=2079 MPa for the outer acrylate coating.

### 3.2 Single-coated Acrylate

Single-coated acrylate is an epoxy acrylate (2-phenoxyethyl acrylate), which is less stiff than the outer coating acrylate mentioned in section 3.1, but it must be approximately ten times stiffer than the inner coating acrylate (based on Table 2). As well as with the double coated acrylate, we have carried out three series of measurements to ensure the

repeatability of our measurements.

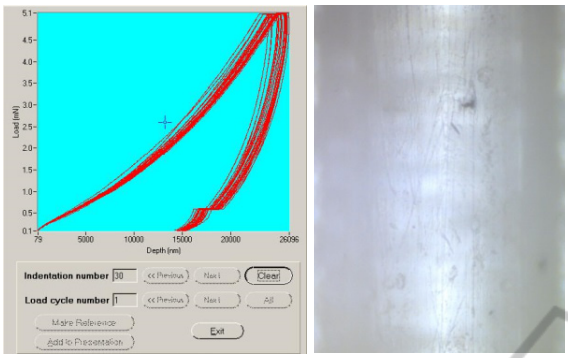


Figure 4: On the left, snapshot of the 30 best loading curves. On the right, a picture of the area selected after nanoindentation, where indents are not visible.

The calculated $E_r$ of the curves on Figure 4 is 9±1 MPa at a *MD* of 25455±548 nm. Substituting this value into equation 2 we obtain $E_s$=7 MPa for the single-coated acrylate.

## 3.3 Fluorinated Acrylate

Fluorinated acrylate is a fluorinated diacrylate oligomer, which can be used either for coating or cladding material of an optical fibre. This coating is normally used for guiding high power lasers, and is the only one compatible for medical applications, according to the United States Pharmacopeia (USP).


Figure 5: On the left, snapshot of the 17 best loading curves. On the right, a picture of the area selected after nanoindentation.

In Figure 5 (right) we can see the indents, which are tiny triangles inside the red rectangle. The fact that the indentations could be marked, might indicate that this material is less elastic than the other two acrylates mentioned in sections 3.1 and 3.2; however the result does not confirm this hypothesis.

In Figure 5 (left) the 17 best loading curves of this material are presented. The calculated $E_r$ is 929±17 MPa at a *MD* of 2665±30 nm. By substituting this $E_r$ value into equation 2 we obtain $E_s$=803 MPa for the fluorinated acrylate.

## 3.4 Polyimide

Polyimide (n-methyl-2-pyrrolidone) is a heat-cured coating, unlike the acrylates which are UV-curing. Since the heat temperature used for curing can vary, any difference could change the mechanical/optical properties of the cured coating; hence the final product can be different from manufacturer to manufacturer. As an example, the polyimide-coated fibres from FiberTech GmbH (like our sample) have a brilliant golden colour (see Figure 6). On the other hand, the polyimide coating from Polymicro Technologies™ has a toasted brown colour, and the refractive index is 1.78. Therefore, the $E_r$ for this coating is expected to be different.

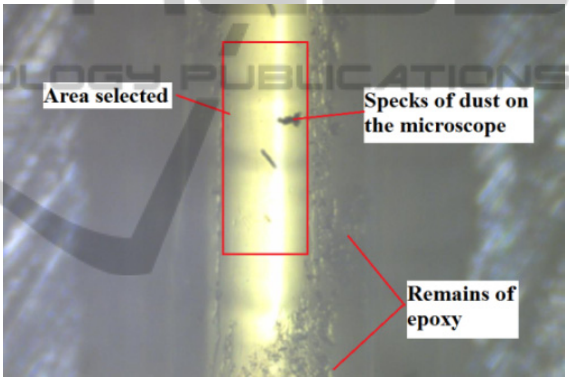


Figure 6: Picture of the selected area for indentation of the polyimide-coated fibre under test.

Noteworthy is that, even if this was the stiffest material, curiously there were no visible indents after the measurement.

Since polyimide coatings are usually thin (our sample has 12 µm of thickness) and it is expected to be the stiffest one, we made a shallower nanoindentation with a *MD*=901±22 nm. In figure 7 the 20 best loading curves are shown with an average $E_r$=5470±205 MPa. Finally, from equation 2 we obtain $E_s$=4861 MPa. This confirms that polyimide is the stiffest coating material that was tested in our experiments.

## 3.5 Silicone

Polydimethylsiloxane, also known as silicone, is a very rubberlike material. Hence, the resulting loading/unloading curve had a very small depth difference (see Figure 8), contrary to the curves of

the previous materials. In Figure 8, the 30 best indents obtained from this material are shown. The curves are together in a very well-defined group. Since it is the most elastic coating among the all mentioned materials in this paper; we increased the depth of the nanoindentation to *MD*=21248±270 nm and the average $E_r$ was 7 MPa.

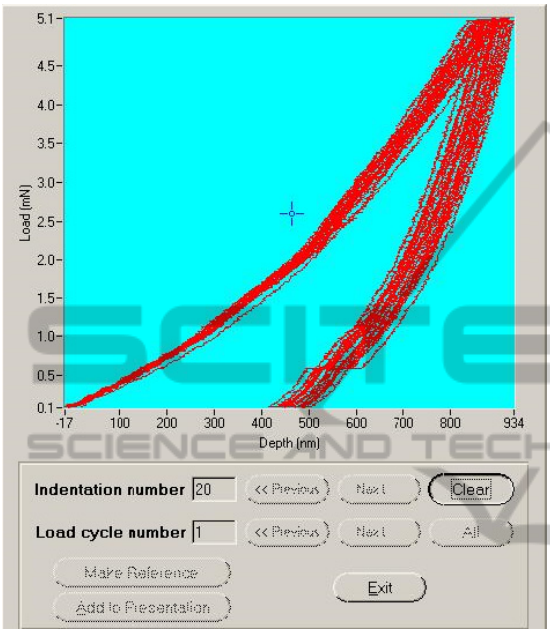


Figure 7: The best 20 loading curves of polyimide coating are shown.

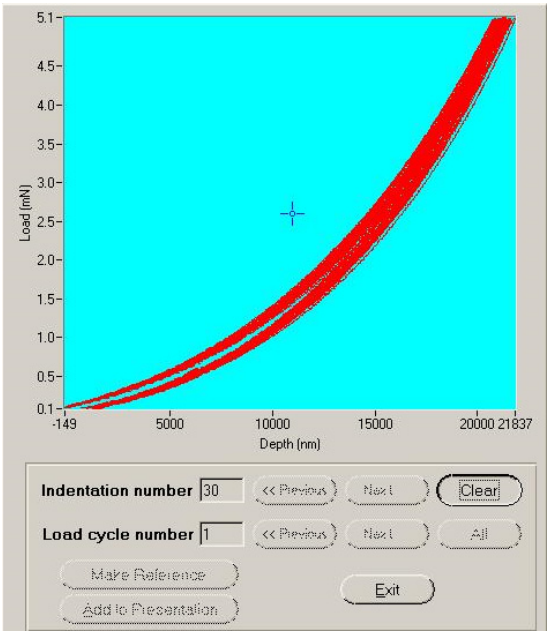


Figure 8: The best 30 loading curves obtained from silicone coating.

Finally, the obtained $E_s$ is 5 MPa, which is surprisingly similar to that of the single-coated acrylate, even if it feels gummy to the touch.

## 3.6 Comparing All Coatings

Table 3 presents a comparison between the best results obtained from each coating. We have confirmed that polyimide is the stiffest material of the all tested materials while silicone is the most elastic one. There are differences between the existing data (Table 2) and our results (Table 3).

Table 3: Comparative table of the best results obtained from Load/Unload curves and equation 2.

| Material | *MD* [nm] | *H* [MPa] | $E_r$ [MPa] | *E* [MPa] |
|---|---|---|---|---|
| Double-coated acrylate | 1507±27 | 123±5 | 2572±57 | 2079±46 |
| Single-coated acrylate | 25455±548 | 0.44±0.0 | 8.80±1.00 | 6.70±0.70 |
| Fluorinated acrylate | 2665±30 | 37.7±1.0 | 929±17 | 803±15 |
| Polyimide | 901±22 | 393±24 | 5470±205 | 4861±182 |
| Silicone | 21248±270 | 1.1±0.01 | 6.60±0.01 | 4.90±0.01 |

For example, *E* of the double-coated acrylate turns out to be twice than the reported value and the single coating acrylate is five times lower than the reported one. However, considering the high sensitivity of the Nanoindenter, the limitations of the method for measuring elastic materials of the order of MPa (see section 2), and curing variations between manufacturers (see section 3.4); the agreement can be considered good and, therefore, the measurements are reliable.

As mentioned in section 1, the purpose of this experiment is to find out how the *E*-value and the attenuation are related. Therefore, we have taken the attenuation data from Padilla Michel, et al. (2012) and our data from Table 3, the resulting graph is shown in Figure 9. In agreement with Padilla Michel, et al. (2012), we have noticed a considerable difference between when the coating refractive index is higher and lower than that of the cladding, which forms two groups.

In order to see clearly how *E*, refractive index and attenuation are related, in Figure 10 we present a graph of the coatings refractive indices as a function of the attenuation. In both graphs (Figures 9 and 10) the group of the higher refractive index (right side) and the group of lower refractive index (left side) are marked. Although, for the group with lower refractive index, *E* does not influences the attenuation, for the group with higher refractive index, it is observed that the higher value of *E*, leads to the lower attenuation value. This is completely contrary to our expectations.

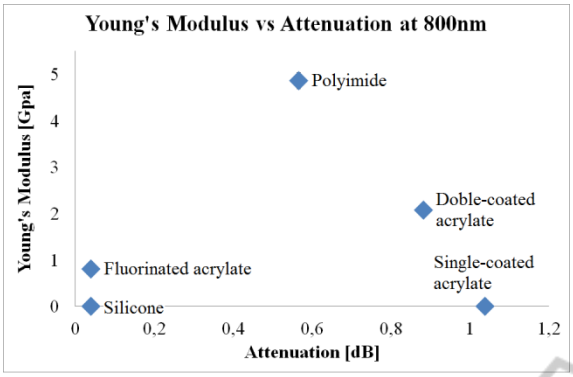


Figure 9: Resulting $E$ of the five coatings tested in this experiment, compared with the attenuation values of Padilla Michel, et al. (2012). The error bars are too small (see Table 3) to be visible in the graph. Plotting $E_r$ instead of $E$ does not change the trend of the graph.

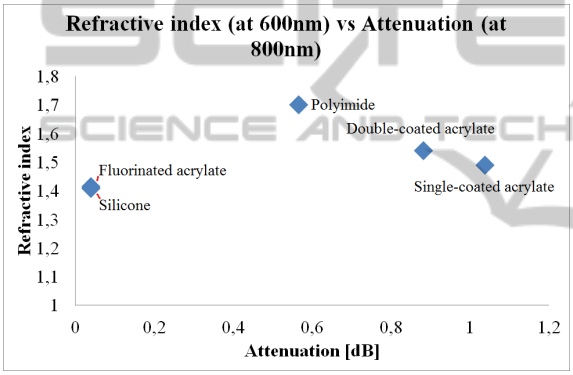


Figure 10: Refractive index versus attenuation. The data were obtained from Padilla Michel, et al. (2012).

Figures 9 and 10 suggest that there are other side effects produced by coating elasticity. Analysing Fig 10, indicates that when the coating material, like acrylate, has a high refractive index value, and a low value of $E$, micro-bendings are produced in the cladding-coating interface leading to an increase in the attenuation (private communication with Dr. Roberto Montanari) while the fibre is bent as reported in Padilla Michel, et al (2012).

## 4 DISCUSSION

The loading curves selected to obtain the $E_r$ reported in Table 3, were those forming a well-defined group. However, in some cases the loading curves from different series of nanoindentation had a considerable difference, even if the same procedure was followed (see Figure 11). These curves were discarded for the calculation of $Er$ and the measurements were repeated. There are different factors that could contribute to these differences:

- The coating area used for indentation, was not perfectly homogenous.
- The 3x10 array of indents could have been made off-side the fibre centre.
- Since the cyanoacrylate used for gluing the fibres and the coatings, both, are translucent; it might be that some indentations were made on an area with debris of glue, which could not be noticed at the moment of selecting the area for indentation.

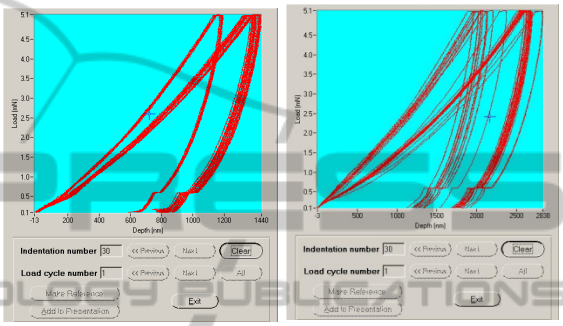

Figure 11: On the left, loading curves of double coating acrylate, showing a group of 10 indents dispersed from the other group. On the right, loading curves of fluorinated acrylate, showing some dispersed curves, as well.

As mentioned in section 3.6, since the micro-bendings produced in the cladding-coating interface increase the attenuation, this parameter should be considered carefully in the case of acrylate. Therefore an alternative method should be used in order to calculate the attenuation without micro-bending losses. As a good alternative we may feed the optical fibres directly through the cladding, thus some cladding modes will interact with the coating without bending the fibre. This will be the next test to corroborate our results and hypothesis.

## 5 CONCLUSIONS

In this paper, we presented the Young's Modulus of the four most used coating materials for NIR fibres. As mentioned above, these mechanical properties are seldom published by the manufacturers; therefore, these results are helpful for a better understanding of the optical fibres performance.

The principle of a waveguide is that the surrounding media (in this case the cladding) must have a refractive index lower than that of the waveguide core in order to keep the modes within it. However, when a waveguide is bent the high order

modes leak into the cladding producing the so-called bending losses. Like explained in Padilla Michel, et al (2012), when the refractive index of the coatings is lower than that of the cladding, the leaky modes go back to the core, due to refractive index differences between layers; therefore, the fibre seems to be insensitive to bending losses independently of the *E* of the coating. However, when the coating refractive index is higher than that of the cladding, the leaky modes are trapped in the coating producing a fibre which is very sensitive to bending losses. In this condition, the *E* of the coating plays an important role in the so-called bending losses.

## ACKNOWLEDGEMENTS

The authors would like to thank the AiF Projekt GmbH (project number KF2014158NT3), the Interne ZV-Cooperation Rome project, for the funds granted, and Dr. Mohamad Zoheidi for providing the fibre samples.

## REFERENCES

Badar, A. H., Maclean, T. S. M., Ghafouri-Siraz, H., Gazey, B. K., 1991. Bent slab ray theory for power distribution in core and cladding of bent multimode optical fibres. *IEE Proceedongs-J*.

Badar, A. H., Maclean, T. S. M., 1991. Transition and pure bending losses in multimode and single-mode bent optical fibers. *IEE Proceedings-J.*

Boechat, A. A. P, Su, D., Hal, D. R., Jones, J. D. C., 1991. Bending loss in large core multimode optical fiber beam delivery systems. *Appl. Opt.*

Durana, G., Zubia, J., Arrue, J., Aldabaldetreku, G., Mateo, J., 2003. Dependence of bending losses on cladding thickness in plastic optical fibers. *Appl. Opt.*

Faustini, L., Martini, G., 1997. Bend loss in single-mode fibers. *IEEE Journal of Lightwave Technology*.

Gambling, W. A., Matsumura, H., Ragdale, C. M., Sammut, R. A., 1978. Measurement of radiation loss in curved single-mode fibres. *Microwaves optics and acoustics*.

Kovacevic, M. S., Nikezic, D., 2006. Influence of bending on power distribution in step-index plastic optical fibers and the calculation of bending loss. *Appl. Opt.*

Mitra, A., Kouzmina, I., Lopez, M., 2010. Thermal stability of the CPC Fiber Coating System. *Corning Incorporated, WP4250.*

Murakami, Y., Tsuchiya, H., 1978. Bending losses of coated single-mode optical fibres. *IEEE Journal of Quantum Electronics*.

Olson, H. G., 2002. *Mechanical and Optical Behaviour of A Novel Optical Fibre Crack Sensor and An Interferometric Strain Sensor*. PhD Thesis submitted at the Massachusetts Institute of Technology.

Padilla Michel, Y., Zoheidi, M., Haynes, R., Olaya, J-C., 2012. Applied stress on coated multimode optical fibres: a different point of view to bending losses". *Proc. SPIE 8450, Modern Technologies in Space- and Ground-based Telescopes and Instrumentation II, 84503F.*

Renner, H., 1992. Bending losses of coated single-mode fibers: A simple approach. *IEEE Journal of Lightwave Technology*.

Valiente, I., Vasallo, C., 1989. New formalism for bending losses in coated single-mode optical fibres. *Electronics Letters.*

Wang, Q., Farrell, G., Freir, T., 2005. Theoretical and experimental investigations of macro-bend losses for standard single mode fibers. *Optics Express*.

Wang, Q., Rajan, G., Wang, P., Farrell, G., 2007. Polarization dependence of bend loss for a standard single-mode fiber. *Optics Express*.